

Collective dynamic length increases monotonically in pinned and unpinned glass forming systems

Rajsekhar Das¹, T. R. Kirkpatrick², and D. Thirumalai¹

¹ *Department of Chemistry, University of Texas at Austin, Austin, Texas 78712, USA and*

² *Institute for Physical Science and Technology,
The University of Maryland, College Park, MD 20742, USA*

The Random First Order Transition Theory (RFOT) predicts that transport proceeds by cooperative movement of particles in domains whose sizes increase as a liquid is compressed above a characteristic volume fraction, ϕ_d . The rounded dynamical transition around ϕ_d , which signals a crossover to activated transport, is accompanied by a growing correlation length that is predicted to diverge at the thermodynamic glass transition density ($> \phi_d$). Simulations and imaging experiments probed the single particle dynamics of mobile particles in response to pinning all the particles in a semi-infinite space or randomly pinning (RP) a fraction of particles in a liquid at equilibrium. The extracted dynamic length increases non-monotonically with a peak around ϕ_d , which not only depends on the pinning method but is different from ϕ_d of the actual liquid. This finding is at variance with the results obtained using the small wave length limit of a four-point structure factor for unpinned systems. To obtain a consistent picture of the growth of the dynamic length, one that is impervious to the use of RP, we introduce a multi particle structure factor, $S_{mp}^c(q, t)$, that probes collective dynamics. The collective dynamical length, calculated from the small wave vector limit of $S_{mp}^c(q, t)$, *increases monotonically* as a function of the volume fraction in glass forming binary mixture of charged colloidal particles in both unpinned and pinned systems. This prediction, which also holds in the presence of added monovalent salt, may be validated using imaging experiments.

I. INTRODUCTION

In a landmark article published in 1964, Aneesur Rahman [1] reported the results of molecular dynamics (MD) simulations investigating the collective motions of atoms in liquid Argon. The simulations, performed using CDC (Control Data Corporation) 3600 computer, consisted of 864 particles at 94.4°K and at the density $1.374 \text{ g}\cdot\text{cm}^{-3}$. For reference, the temperature and density at the triple point of Argon are 80.8°K and $1.417 \text{ g}\cdot\text{cm}^{-3}$, respectively. In retrospect, it is clear that the 1964 study laid the foundation for using MD simulations in ways that were unimaginable at that time. Rahman also developed the theoretical basis of MD simulations and applied them to a bewildering range of problems, spanning phase transitions in solids [2, 3], lattice gauge simulations [4], structure of molecular fluids, especially liquid water [5, 6], aspects of glasses [7, 8], and much more. His pioneering work with Rossky and Karplus showed that MD [9] could be used to simulate peptides and proteins in aqueous solutions, which have, over the last nearly five decades, provided quantitative insights into their dynamics that are often difficult to obtain from experiments alone. These and other studies by Rahman, which are far too many to enumerate here, propelled MD as an indispensable branch of study in physical sciences and biology.

Not surprisingly, molecular dynamics simulations have been instrumental in testing different theories of the structural glass transition (SGT) [10–15]. Given that current the literature is vast, we cite only a few references including some recent reviews [16–21]. Among the contenders, the Random first-order transition theory (RFOT) [11, 12, 15, 22, 23] has been successful in explaining most of the phenomena associated with SGT. (1) RFOT predicts that there ought to be two transitions as the system is cooled by lowering the temperature, T or compressed by increasing the density. Upon supercooling (or compressing) a liquid, a rounded dynamical transition occurs at the temperature $T \approx T_d$ (or ϕ_d) (T_d (ϕ_d) is a roughly the mode-coupling transition temperature (density)). The liquid is pictured as a “mosaic” of correlated amorphous domains at volume fractions exceeding ϕ_d . Above ϕ_d transport occurs by activated processes, although typically barrier limited transport takes place even before ϕ_d is reached because of the rounded nature of the transition at ϕ_d . The driving force for transport, above ϕ_d , is entropic in origin and is opposed by scale dependent surface tension [11]. The latter is a unique feature of RFOT. At a lower temperature or higher density a thermodynamic ideal glass transition occurs. (2) Due to the emergence of multiple

mosaic domains, the dynamics, which become heterogeneous around ϕ_d , are accompanied by a growth in the dynamic correlation length. RFOT predicts both the static and dynamic correlation lengths should diverge at the ideal glass transition.

Estimation of the dynamic or static correlation length using MD simulations is challenging, even for $\phi \sim \phi_d$ (ϕ is the volume fraction in the colloidal particles) because of the difficulty in equilibrating the sample within the simulation time. The use of the particle pinning technique (an uncontrolled externally imposed disorder that breaks translational invariance) [14, 24–30], makes it possible to obtain equilibrium data close to or even above ϕ_d . However, estimates of the dynamic length close to ϕ_d (or below T_d) using the RP method using simulations and experiments have led to contradictory results. By pinning all the particles in a binary mixture of harmonic spheres in a semi-infinite space the response in the other half-space was probed [31]. The use of a frozen amorphous wall is a generalization of the point-to-set method [32–34] for estimating the dynamic length. The calculated length (ξ_d^s) using single particle dynamics changed *non-monotonically* with a peak at $\approx T_d$ as T is decreased.

Flenner and Szamel (FS) [35] simulated the same model without RP and calculated ξ_d by fitting the low wave vector behavior of the four-point dynamic structure factor $S_4^s(q, t)$ to the Ornstein-Zernike equation (OZ). In contrast to the previous simulations [31], they found that ξ_d^s increases *monotonically*. As pointed out by FS, the use of RP, especially the amorphous wall, elicits (unknown) non-linear response on the dynamics of the unpinned particles. For this reason, it is unclear if the RP method faithfully reports the dynamics of unperturbed bulk liquid [35].

Subsequent simulations using a binary mixture of particles interacting via harmonic [36] and Lennard-Jones (LJ) potentials [37] have added to the discussion on the usefulness of the RP method. By placing two walls separated by a distance, d , it was shown that the temperature at which ξ_d attains a maximum is d dependent [36]. More strikingly, the maximum vanishes if the walls are smooth. Simulations of the LJ system revealed that ξ_d , determined by using the point-to-set method [33], saturates when $T > T_d$ without showing the expected non-monotonic behavior.

Two insightful experiments that support the thermodynamic origin of the SGT appeared after the simulations [31, 35]. (1) An experimental realization of a frozen wall of particles was achieved by a holographic optical tweezer setup [38]. Video microscopy experiments

on a binary mixture of micron-sized neutral polystyrene particles in two dimensions were used to measure the response of the frozen amorphous wall on the dynamics as a function of the distance from the wall. By fitting the z (distance from the wall) dependence of the time-dependent decay of the self part of the overlap function, it was found that the inferred dynamic length increases non-monotonically as a function of the packing fraction, which was in accord with the simulation results [31], obtained by changing the temperature. (2) Because randomness is self-generated in glasses [39], it would be prudent to realize pinned configurations by probing the response of motile particles to “slow” particles that relax on times that are much greater than the typical relaxation time, τ_α . Such an experiment was performed on a binary mixture of colloidal polystyrene particles [40] in three dimensions. They first identified particles that mimic pinned particles (self-induced pinning) for which the relaxation time is on the order of $(5-7)\tau_\alpha$. The extracted ξ_d also changes non-monotonically, with a maximum value $\xi_d \approx 10\sigma_s$ ($\sigma_s = 1.05\mu m$ is the size of the smaller particle) as the volume fraction increases. It is worth pointing out that in both these experiments there is only one data point in the ξ_d versus packing fraction plots after the maximum near ϕ_d (Fig. 2c in [40] and Fig. 3a in [38]). The results were interpreted in terms of changes in shapes of the mosaic domains [41] as ϕ approaches ϕ_d . Despite changing the pinning protocol the qualitative conclusions in the three studies [31, 38, 40] are similar - the dynamical length increases non-monotonically reaching a maximum at a temperature or density that is close to the dynamic transition point of the pinned system.

The foregoing summary of the experimental and simulation results shows that the extraction of ξ_d using the RP method and its interpretation is not straight forward. To obtain consistent results for the dynamic length, without and with RP, we introduce a two-point overlap function, which has been used to distinguish between the folded and unfolded states of globular proteins [42, 43]. Using simulations of binary mixtures of charged colloidal suspensions [44], which form classical Wigner glasses [45], we calculated the collective multi-point dynamic structure factor $S_{mp}^c(q, t)$, describing the fluctuations in the two-point overlap function, as well as the self-part, $S_4^s(q, t)$. The main findings may be summarized as follows. (1) Collective length (referred to as ξ_d^c here on) obtained by fitting the low q part of $S_{mp}^c(q, t)$ to the OZ equation grows *monotonically* as a function of ϕ in both pinned and unpinned systems. In contrast, ξ_d^s calculated using the low q dependence of the self part of four-point dynamic structure factor $S_4^s(q, t)$ grows *non-monotonically* with a peak near ϕ_d . (2) Strik-

ingly, for the unpinned liquid, the length scale calculated from both $S_4^s(q, t)$ and $S_4^c(q, t)$ gives quantitatively identical values, exhibiting monotonic growth as a function of ϕ . On the other hand, in a pinned system, ξ_d^s (ξ_d^c) increases non-monotonically (monotonically). (3) For the pinned liquids we show that the collective dynamics become increasingly important as ϕ increases. Single particle dynamics, used in all previous studies [31, 38], underestimates correlated dynamics, which is especially relevant as ϕ approaches ϕ_d . (4) At the onset of collective dynamics, which occurs at $\phi < \phi_d$ there is a dynamic crossover that can be probed using RP. The relaxation time τ_α as a function of ξ_d^c changes from $\tau_\alpha \sim \exp[k\xi_d^c]$ to $\tau_\alpha \sim \exp[k(\xi_d^c)^{3/2}]$ [35] in accord with the predictions of RFOT [11]. The $(\xi_d^c)^{3/2}$ scaling follows from very general arguments [22] and is independent of the method used to compute the length as function of ϕ .

II. MODELS AND METHODS

Charged colloids: We simulated a binary mixture of highly charged micrometer-sized colloidal particles [44, 46, 47], which form classical Wigner glasses [45], by randomly pinning a fraction (ρ_{pin}) of particles at their equilibrium positions. We also simulated unpinned ($\rho_{\text{pin}} = 0$) systems. The 50:50 binary mixture is composed of two types of particles with diameters $a_1 = 5.5\mu m$ and $a_2 = 1.1\mu m$.

The particles, separated by a distance r_{ij} , interact via the Derjaguin-Landau-Verwey-Overbeek potential [48–52],

$$V_{ij}(r_{ij}) = \frac{e^2 Z_i Z_j}{4\pi\epsilon} \left(\frac{\exp[\kappa a_i]}{1 + \kappa a_i} \right) \left(\frac{\exp[\kappa a_j]}{1 + \kappa a_j} \right) \left(\frac{\exp[-\kappa r_{ij}]}{r_{ij}} \right), \quad (1)$$

where Z_i , κ and ϵ are the valence of the charged colloids, inverse Debye-Hückel screening length, and the dielectric constants, respectively. The values of Z_i for the large and small particles are 600 and 300, respectively. The dielectric constant $\epsilon = \epsilon_0 \epsilon_r$, where ϵ_0 is the free space permittivity, and ϵ_r is the relative permittivity. At the temperature $T = 298K$, we set the dielectric constant to $\epsilon_r = 78$. The inverse Debye-Hückel screening length κ is,

$$\kappa^2 = \frac{e^2}{\epsilon K_B T} \left(\rho_c z_c^2 + \sum_{i'}^n \rho_{i'} z_{i'}^2 \right), \quad (2)$$

where ρ_c and z_c are the number density and valence of the counterions, respectively, ρ_i and z_i are the number density and the valence of the added salt, respectively, and k_B is the

Boltzmann constant. For monovalent ions, $|z_c| = 1$ and $\rho_c = \rho_1 Z_1 + \rho_2 Z_2$, where ρ_1 and ρ_2 are the number density of the small and the large particles respectively. In the presence of added monovalent ions, $\rho_{add} = \sum_{i'}^{n=2} \rho_{i'}$, we define a relative excess ion density,

$$\rho_r = \frac{\rho_{add}}{\rho_c}. \quad (3)$$

In the current work, we set $\rho_r = 0$ and 5. The effective range of interaction increases with decreasing ϕ and ρ_r [44]. The interaction potential $V_{ij}(r)$ is truncated at a distance r_c , determined by the condition $V_{ij}(r_c) = 0.001k_B T$. Because the interaction potential is not as long-ranged as the Coulomb potential, we did not find the need to use Ewald summation. The thermodynamic variable in the simulations is the volume fraction,

$$\phi = \frac{4\pi}{3L^3} (N_1 a_1^3 + N_2 a_2^3). \quad (4)$$

Total number of particles, $N = N_1 + N_2$, is typically 10,000.

Methods

We performed Brownian dynamics (BD) simulations by integrating the equation of motion,

$$\frac{d\vec{r}_i(t)}{dt} = -\nabla_{\vec{r}_i} U(\vec{r}_1, \dots, \vec{r}_N) \frac{D_{i,0}}{K_B T} \delta t + \sqrt{2D_{i,0}} \vec{R}_i(t), \quad (5)$$

where, $\vec{r}_i(t)$ is the position of the i^{th} particle at time t , $U(\vec{r}_1, \dots, \vec{r}_N) = \sum_{i \neq j} V_{ij}(r_{ij})$. The integration time step is δt , and $D_{i,0}$ is the bare diffusion constant of the i^{th} particle. The bare diffusion constants for the small and the large colloidal particles are chosen as $4.53 \mu m^2/s$ and $2.24 \mu m^2/s$, respectively. We calculated $D_{i,0}$ using the Stokes-Einstein relation, $D_{i,0} = \frac{k_B T}{6\pi\eta a_i}$, where $\eta = 0.89$ mPa s for water. The $\vec{R}_i(t)$ on the right-hand side of the Eqn. (5) is a random noise, which satisfies $\langle \vec{R}_i(t) \vec{R}_j(t') \rangle = 6D_{i,0} \delta_{ij} \delta(t - t')$, where δ_{ij} is the Kronecker delta and $\delta(t - t')$ is the Dirac delta function. The integration time step δt is set to $10 \mu s$ for $\rho_r = 0$ and $1 \mu s$ for $\rho_r = 5$ to ensure numerical accuracy [44]. The relative excess ion density $\rho_r = 5$ corresponds to ≈ 0.44 millimolar salt concentration.

We reported simulation results for these systems in a previous study [44] without RP. The calculated values of ϕ_d for $\rho_r = 0$ is ≈ 0.10 and for $\rho_r = 5$ is ≈ 0.36 . The increase in ϕ_d reflects a decrease in the range of DLVO potential.

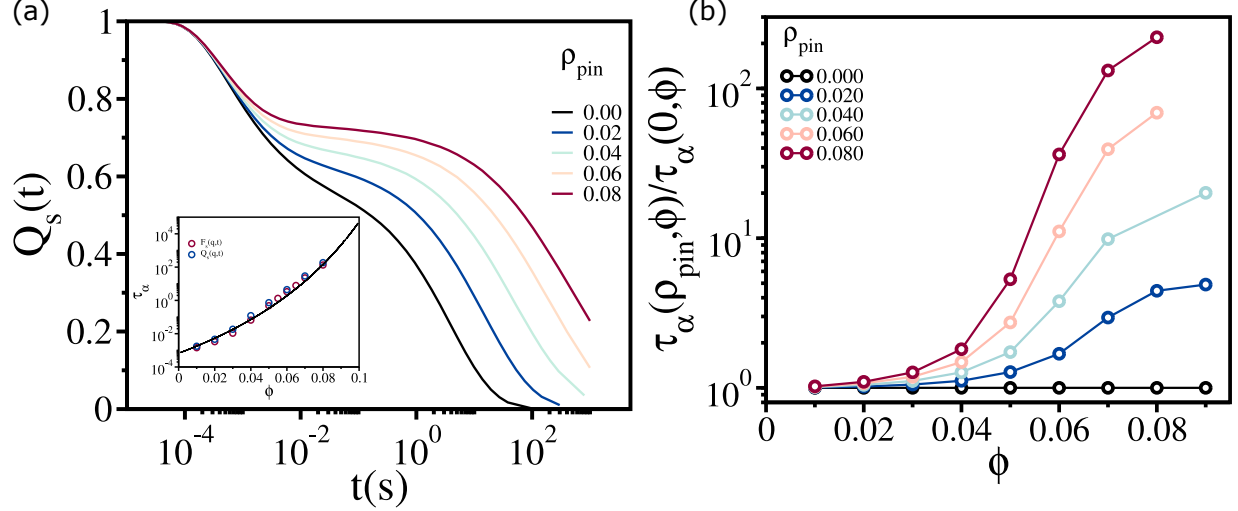


FIG. 1: **Structural relaxation time in randomly pinned systems:** (a) Self overlap function $Q_s(t)$ as function of t for $0.00 \leq \rho_{\text{pin}} \leq 0.08$ at $\phi = 0.09$ for $\rho_r = 0$. Inset compares τ_α calculated using $Q_s(t)$ and the self-intermediate scattering function, $F_s(q, t)$, with $q = 2\pi/d_{\text{ave}}$. (b) $\tau_\alpha(\rho_{\text{pin}}, \phi)/\tau_\alpha(0, \phi)$ as a function of ϕ for $0.00 \leq \rho_{\text{pin}} \leq 0.08$ and $\rho_r = 0$.

III. RESULTS & DISCUSSIONS

Pining enhances the relaxation times: We calculated the relaxation time, τ_α , using the decay of the self structural overlap function,

$$Q_s(t) = \frac{1}{N - N_p} \left[\left\langle \sum_{i=1}^{N-N_p} w_i(t) \right\rangle \right], \quad (6)$$

where $[\langle \dots \rangle]$ is the ensemble average and average over different time origins, N is the total number of particles, and N_p is the total number of pinned particles. The overlap function, $w_i(t) = \Theta(a - |\vec{r}_i(t) - \vec{r}_i(0)|)$, describes the duration for which particle i remains within a distance a at time t given that it is within a at $t = 0$; $\vec{r}_i(t)$ is the position of a particle at time t . The Heaviside function, $\Theta(x)$, is unity if $|\vec{r}_i(t) - \vec{r}_i(0)| \leq a$ and zero otherwise. Thus, $Q_s(t)$ measures the average number of particles that do not move a distance of a from their original position after a time t . These particles could be referred to as slow particles. Note that, $Q_s(t)$ has similar information as the self-intermediate scattering function $F_s(q, t) = N^{-1} \left\langle \sum_{i=1}^N e^{-i \cdot [\vec{r}_i(t) - \vec{r}_i(0)]} \right\rangle$ [53]. With the choice of $a = 0.3d_{\text{ave}}$ [44], we find that $\langle Q_s(t) \rangle$ decays with a relaxation time τ_α , which coincides with the time scale of decay of the self intermediate scattering function $F_s(q, t)$ with $q = 2\pi/d_{\text{ave}}$ (Fig. 1 (a) inset). The volume-

averaged value of the diameter of the charged colloids is $d_{\text{ave}} = 2 \frac{\phi_1 a_1 + \phi_2 a_2}{\phi_1 + \phi_2}$ with ϕ_1 and ϕ_2 being the volume fractions of small and large colloids respectively. The structural relaxation time, τ_α , is calculated using $Q_s(t = \tau_\alpha) = 1/e$.

Several studies [29, 54, 55] have shown that, τ_α , increases sharply as the fraction, ρ_{pin} , of the pinned particles increases (Fig. 1 (a) and (b)). At $\rho_{\text{pin}} = 0.08$, it is ~ 300 times slower compared to the unpinned case at $\phi = 0.09$. Therefore, at a fixed ϕ increasing ρ_{pin} is effectively equivalent to compressing the liquid.

Dynamic heterogeneity: When a glass-forming liquid is compressed, the dynamics become progressively heterogeneous [12, 15, 56, 57]. The degree of dynamic heterogeneity may be characterized by the fluctuations in the self part of the two-point correlation function [58, 59],

$$\chi_4^s(t) = (N - N_p) [\langle Q_s(t)^2 \rangle - \langle Q_s(t) \rangle^2], \quad (7)$$

where $\langle \dots \rangle$ represent the ensemble average and average over different time origins.

We find that the four-point function $\chi_4^s(t)$ grows non-monotonically as a function of t when ϕ and ρ_{pin} increase, which indicates that the initial correlation between particles is minimal and grows with time with a maximum at intermediate times. The maximum in $\chi_4^s(t)$, whose amplitude is χ_4^P , appears at $t \simeq \tau_\alpha$. The peak height χ_4^P is directly related to the degree of dynamic heterogeneity [60–62]. Fig. 2 (a) shows that at $\rho_{\text{pin}} = 0.0$, χ_4^P grows monotonically as the liquid is compressed toward ϕ_d ($\phi_g \approx 0.10$ [44]), which is a signature that the dynamics is increasingly heterogeneous as ϕ is increased.

When the number of pinned particles increases, the maximum in the $\chi_4^s(t)$ does not increase monotonically as the ϕ increases (Fig. 2 (b) and (c)). For $\rho_{\text{pin}} > 0.02$, χ_4^P as a function of ϕ exhibit non-monotonic behavior (Fig. 2 (d)). It increases until ϕ_N (ϕ_N is the packing fraction where non-monotonicity appears) and then decreases upon further increases in ϕ . Moreover, for $\phi > \phi_N$, χ_4^P systematically decreases as ρ_{pin} increases. Similar observations were made in earlier works [54, 63, 64]. However, the reason for the non-monotonic behavior of χ_4^P with the increase in ϕ is still unclear.

To assess if the observed behavior is an effect of finite system size, we performed additional simulations by varying N . The qualitative behavior is independent of the system size for unpinned and pinned liquids (Fig. 2 (e) & (f)). The results shown in Fig. 2 apparently suggest that when the number of pinned particles increases, the dynamically correlated

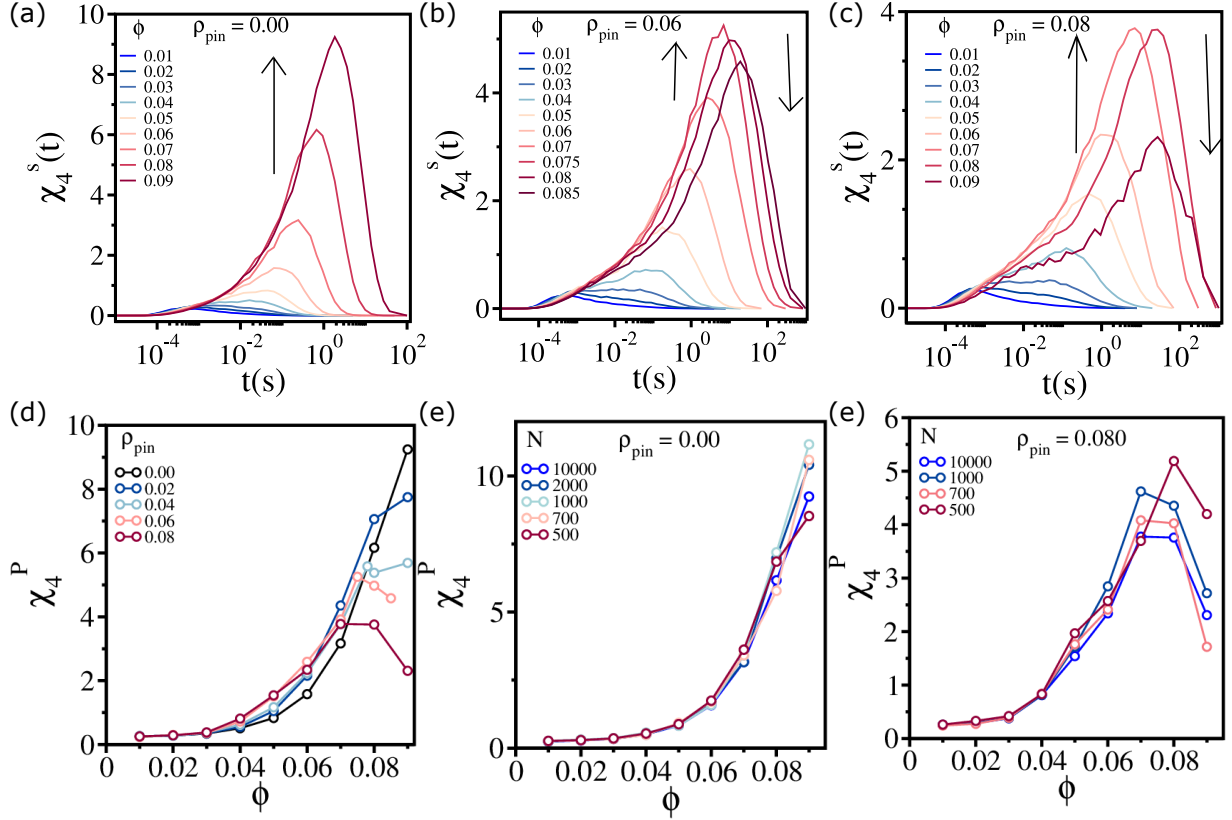


FIG. 2: **Non-monotonic growth of $\chi_4^s(t)$:** Four-point dynamic susceptibility $\chi_4^s(t)$ as function of t for $0.01 \leq \phi \leq 0.09$ at $\rho_{\text{pin}} = 0.0$ (a), $\rho_{\text{pin}} = 0.06$ (b) and $\rho_{\text{pin}} = 0.08$ (c). The arrows in the upward direction indicate the peak in the $\chi_4^s(t)$ increases whereas the downward arrows indicate it decreases. (d) The peak value of $\chi_4^s(t)$ (χ_4^P) as a function of ϕ for $0.0 \leq \rho_{\text{pin}} \leq 0.08$. (e) χ_4^P as a function of ϕ for $500 \leq N \leq 10,000$ with $\rho_{\text{pin}} = 0.0$. (f) Same as (e) except it is for $\rho_{\text{pin}} = 0.08$.

region exhibits non-monotonic behavior as a function of ϕ , as assessed by $\chi_4^s(t)$.

Dynamic length from single particle dynamics: To quantify the length scale associated with the dynamically correlated regions, we first investigated the small wave-number dependence of the self part of the four-point dynamic structure factor $S_4^s(q, t)$ [65],

$$S_4^s(q, t) = (N - N_p) [\langle W_0^s(q, t) W_0^s(-q, t) \rangle - \langle W_0^s(q, t) \rangle^2], \quad (8)$$

where,

$$W_0^s(q, t) = \frac{1}{N - N_p} \sum_j^{N - N_p} w_j(t) \exp[-i\vec{q} \cdot \vec{r}_j(0)]. \quad (9)$$

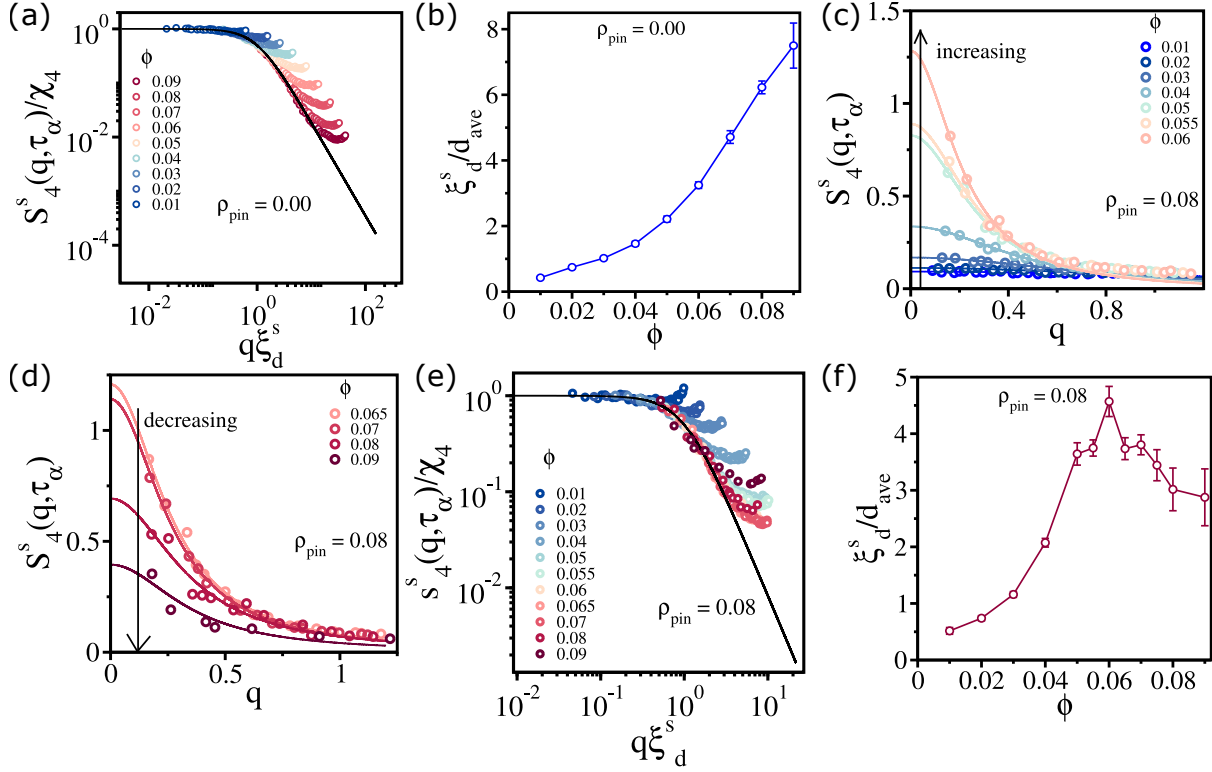


FIG. 3: **Non-monotonic growth of the dynamical length from self-correlation function:**

(a) $S_4^s(q, \tau_\alpha)$ scaled by χ_4 as a function of $q\xi_d^s$ for $0.01 \leq \phi \leq 0.09$ at $\rho_{\text{pin}} = 0.0$. The solid line is the fit to Eqn. (10). (b) ξ_d^s obtained from the OZ fit in (a), as a function of ϕ . (c) $S_4^s(q, \tau_\alpha)$ as a function of q for $0.01 \leq \phi \leq 0.06$ at $\rho_{\text{pin}} = 0.08$. (d) Same as (c), except it is for $0.065 \leq \phi \leq 0.09$. (e) Same as (a) but for $\rho_{\text{pin}} = 0.08$. (f) ξ_d^s as a function of ϕ for $\rho_{\text{pin}} = 0.08$.

In Eq. 9, $w_j(t) = \Theta(a - |\vec{r}_j(t) - \vec{r}_j(0)|)$ with $a = 0.3d_{\text{ave}}$. The small q dependence of $S_4^s(q, \tau_\alpha)$ is well described by the Ornstein-Zernike (OZ) [53, 65–67] equation,

$$S_4^s(q, \tau_\alpha) \simeq \frac{\chi_4}{1 + q^2 \xi_d^s{}^2}, \quad (10)$$

where ξ_d^s and χ_4 are fit parameters, ξ_d^s is the size of the dynamically correlated region. The coefficient, χ_4 in Eqn. (10), is the value for an infinite system, which is interpreted as the average number of particles belonging to the dynamically correlated region.

In Fig. 3 (a), we show the OZ fit to the $S_4^s(q, \tau_\alpha)$ to estimate the dynamic length scale for $\rho_{\text{pin}} = 0.0$. The calculated ξ_d^s grows *monotonically* as a function of ϕ (Fig. 3 (b)), which accords well with FS findings for the harmonic system [35]. However, for $\rho_{\text{pin}} = 0.08$,

$S_4^s(q, \tau_\alpha)$ as a function of q increases with ϕ for $\phi \leq 0.06$, and decreases upon further increase in ϕ (see Fig. 3 (c) & (d)). The calculated ξ_d^s from the OZ fit (Fig. 3 (e)) grows *non-monotonically* as a function of ϕ (Fig. 3 (f)). A similar non-monotonic dynamic length scale was reported in previous computational studies [31, 36, 68] using different interaction potentials as well as in experiments [38, 40].

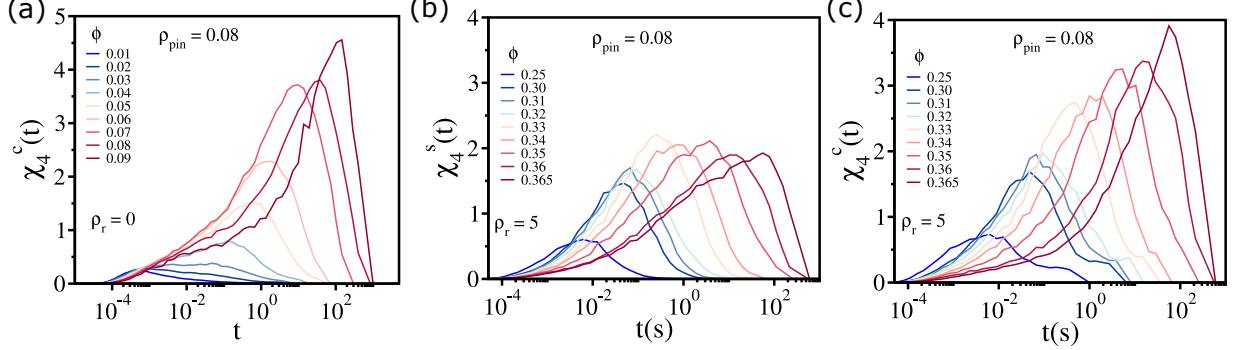


FIG. 4: **Monotonic growth of peak in χ_4^c :** (a) The collective four-point dynamic susceptibility $\chi_4^c(t)$ as a function of t for $0.01 \leq \phi \leq 0.09$ with $\rho_{\text{pin}} = 0.08$ for $\rho_r = 0$. (b) The self $\chi_4^s(t)$ as a function of t for $0.25 \leq \phi \leq 0.365$ with $\rho_{\text{pin}} = 0.08$ for $\rho_r = 5$. (c) Same as (b) but for $\chi_4^c(t)$.

It is important to emphasize that in the discussion so far, we have calculated the susceptibility ($\chi_4^s(t)$) and the length scale (ξ_d^s) from the self part of the correlation function, which is commonly used in the literature [54, 63, 64]. However, the self part of the correlation function does not account directly for how single particle affects the dynamics of other particles over time especially as ϕ approaches ϕ_d . We find that the peak of collective $\chi_4^c(t)$ increases monotonically (see Fig. 4). Therefore, one needs to investigate the collective correlation functions to understand the dynamics of glass-forming liquids correctly [14, 69, 70].

Dynamic length using multi-particle correlation function: We calculated the small wave-number dependence of the collective multi-particle dynamic structure factor $S_{mp}^c(q, t)$,

$$S_{mp}^c(q, t) = (N - N_p) [\langle W_0^c(q, t) W_0^c(-q, t) \rangle - \langle W_0^c(q, t) \rangle^2], \quad (11)$$

where,

$$W_0^c(q, t) = \frac{1}{N - N_p} \sum_{k \neq j}^{N - N_p} w_{kj}(t) \exp[-i\vec{q} \cdot \vec{r}_j(0)]. \quad (12)$$

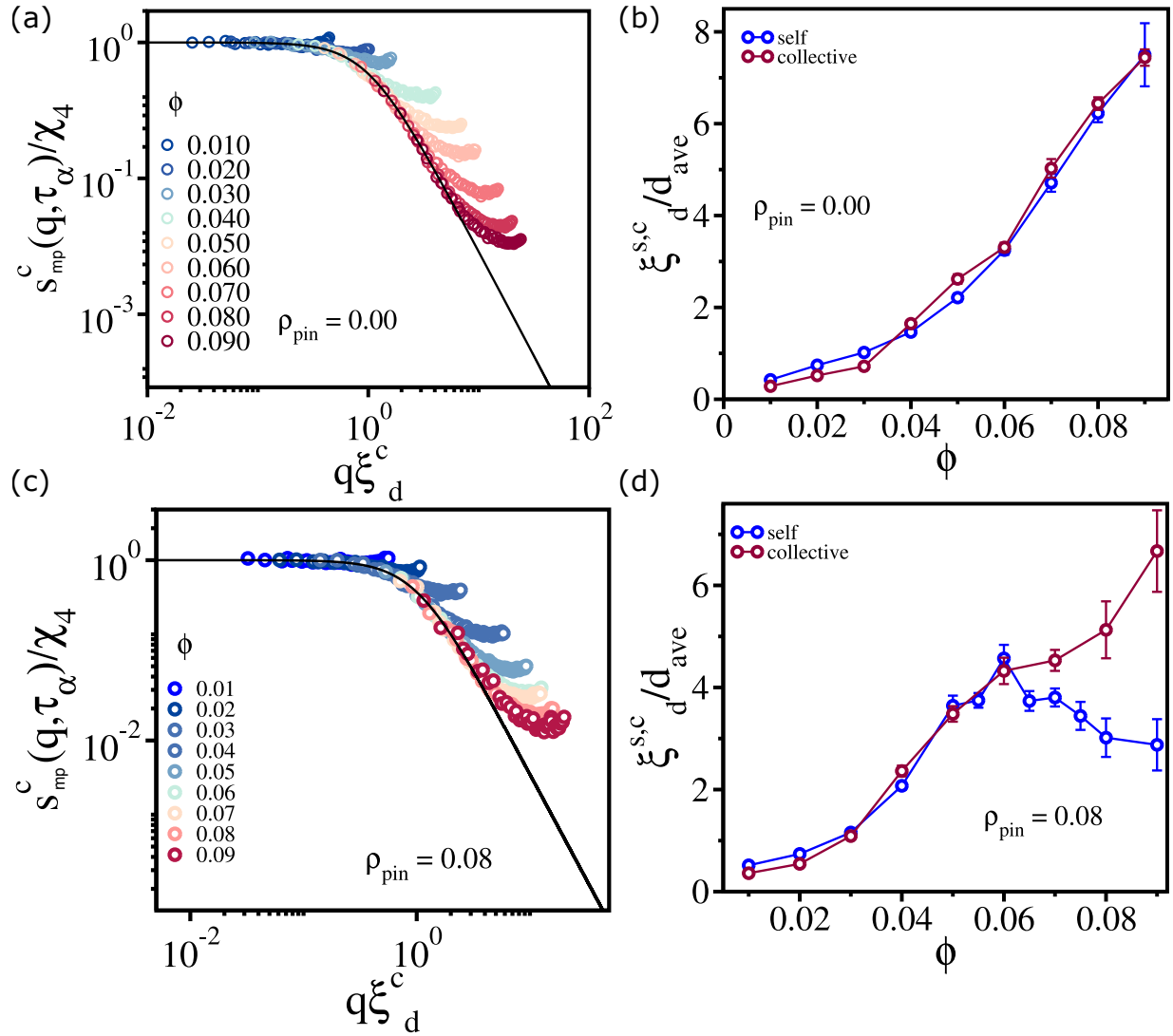


FIG. 5: **Monotonic growth of dynamical length from collective correlation function:** (a) $S_{mp}^c(q, \tau_\alpha)$ scaled by χ_4 as a function of $q\xi_d^c$ for $0.01 \leq \phi \leq 0.09$ at $\rho_{pin} = 0.0$. The solid line is the fit to Eqn. (10). (b) ξ_d^c obtained from the fitting in (a) and ξ_d^s obtained from Fig. 3 (b) as a function of ϕ . (c) Same as (a), but it is for $\rho_{pin} = 0.08$. (d) Comparison of length scale ξ_d^c obtained from (c) and ξ_d^s from Fig. 3 (f).

The two-point overlap function,

$$w_{kj}(t) = \Theta(a - |\vec{r}_k(t) - \vec{r}_j(0)|) \quad (13)$$

is an order parameter that was introduced in protein folding to distinguish between folded and unfolded states of globular proteins [43]. The OZ fit (see Appendix for details) to the

collective dynamic structure factor $S_{mp}^c(q, t)$ used to calculate ξ_d^c for $\rho_{\text{pin}} = 0.0$ is shown in Fig. 5 (a). The length scale calculated from the $S_{mp}^c(q, t)$ is quantitatively similar to that estimated using $S_4^s(q, t)$ (Fig. 5 (b)). However, for $\rho_{\text{pin}} = 0.08$, ξ_d^c calculated using $S_{mp}^c(q, t)$ grows *monotonically* as a function of ϕ , whereas the ξ_d^s exhibits a *non-monotonic* behavior (Fig. 5 (d)). Therefore, we conclude that the self part of the correlation underestimates the overall correlation between particles, resulting in the *non-monotonic* growth of ξ_d^s at non-zero values of ρ_{pin} .

The maximum in ξ_d^s in Fig. 3 (f) is at $\phi \approx \phi_d$, estimated by fitting $\xi_d^c \sim (\phi_d - \phi)^{-\gamma}$ (or to the τ_α as function of ϕ data). We estimate $\phi_d \simeq 0.064$ at $\rho_{\text{pin}} = 0.08$, which is less than the value at $\rho_{\text{pin}} = 0.0$ ($\phi_d \simeq 0.10$, see Table I in Ref [44]). This implies that collective dynamics is negligible at $\phi \lesssim \phi_d$ and become important only when ϕ exceeds ϕ_d but still less than ϕ_g . It is worth noting that free energy barrier limited transport starts to be prominent even before ϕ_d [71]. We should emphasize that, as highlighted by FS [35], the previously utilized generalized point-to-set method captures the nonlinear response of the pinned particles on the dynamics of the unpinned particles, rather than directly measuring the actual multi-particle dynamic correlations. In contrast, the collective $S_{mp}^c(q, t)$ quantifies how slow-moving particles are correlated with one another over a length scale that is *intrinsic* to the liquid.

It is important to note that the collective length scale ξ_d^c for the unpinned system is larger than ξ_d^c for pinned system (compare Fig. 5 (b) and (d)). This is a result of pinned particles altering the system drastically– the pinned system becomes “strong” liquids (Fig. 6). Therefore, one would expect a slow evolution of the length scale in the pinned system.

To quantify the extent to which $S_4^s(q, t)$ underestimates the overall correlation between particles over time, we first define the collective overlap function $Q_c(t)$,

$$\begin{aligned} Q_c(t) &= \frac{1}{N - N_p} \left[\left\langle \sum_{i,j=1}^{N-N_p} w_{ij}(t) \right\rangle \right] \\ &= \frac{1}{N - N_p} \left[\left\langle \sum_{i=1}^{N-N_p} w_i(t) \right\rangle \right] + \frac{1}{N - N_p} \left[\left\langle \sum_{i \neq j}^{N-N_p} w_{ij}(t) \right\rangle \right] \\ &= Q_S + Q_D. \end{aligned} \tag{14}$$

Next, we define $Q_{\text{DR}} = \frac{Q_D}{Q_c}$. For $\rho_{\text{pin}} = 0.0$, we find that at $t \simeq \tau_\alpha$, the contribution of Q_D to the overall correlation is almost negligible even at $\phi = 0.09$ (Fig. 7 (a)). As a consequence,

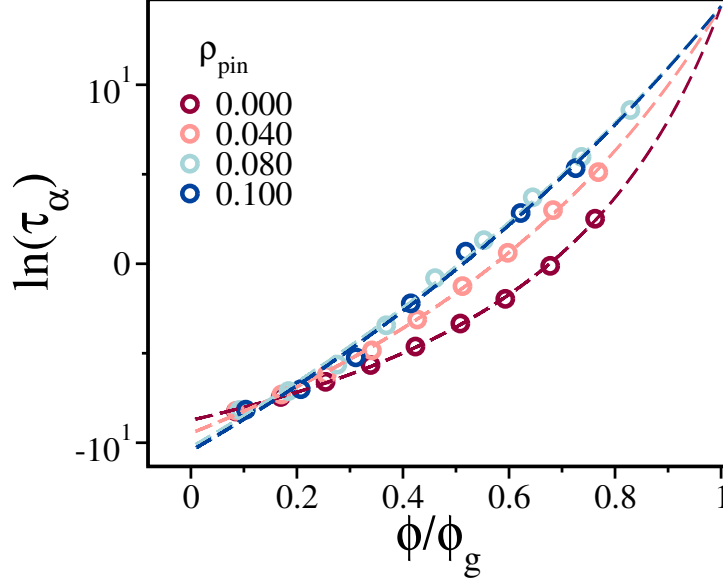


FIG. 6: **Angell plot for various pinning fractions:** Logarithm of the relaxation time τ_α as a function ϕ/ϕ_g for $\rho_r = 0$. Here $N = 1000$.

the length scale estimated from the collective correlation function $S_{mp}^c(q, t)$ and the self-correlation function $S_4^s(q, t)$ do not differ (Fig. 5 (b)). This is also reflected in Q_{DR} at τ_α , which increases only by $\sim 5\%$ at $\phi = 0.09$. In contrast at $\rho_{pin} = 0.08$, Q_D is significant ($\gtrsim 20\%$ for $\phi \geq 0.08$) at $t = \tau_\alpha$ when $\phi \geq 0.06$ (Fig. 7 (b)). Strikingly, for $\phi \geq 0.06 \approx \phi_d$, the single particle length ξ_d^s calculated using $S_4^s(q, t)$ starts to decrease upon increasing ϕ (Fig. 3 (f)).

To illustrate the importance of two-point functions, we define a particle as self-correlated for which $Q_S > 0.0$ at $t = \tau_\alpha$ and distinctly correlated if $Q_D > 0.0$ (Eqn. (14)). As shown in Fig. 7 (c)-(f), a significant number of particles become distinctly correlated when $\phi \geq 0.06$, which is signaled by the increase in Q_{DR} . We identify this value of ϕ as the onset of collective dynamics. After the onset of the collective dynamics, one would see an apparent non-monotonic dynamic length scale if calculated from the self part of the correlation function (Fig. 5 (f) and Fig. 9 (b)).

Dynamic crossover: The dependence of ξ_d^s for $\rho_{pin} = 0.08$ with a maximum at $\phi \sim 0.06$ suggests that there is a change in the dynamics, as noted previously [35]. Interestingly, the onset of collective dynamics is also reflected in a log-log plot of τ_α as a function of ξ_d^c (Fig. 8 (b)). For $\phi \leq 0.06$ (moderately compressed region), the data is well described by

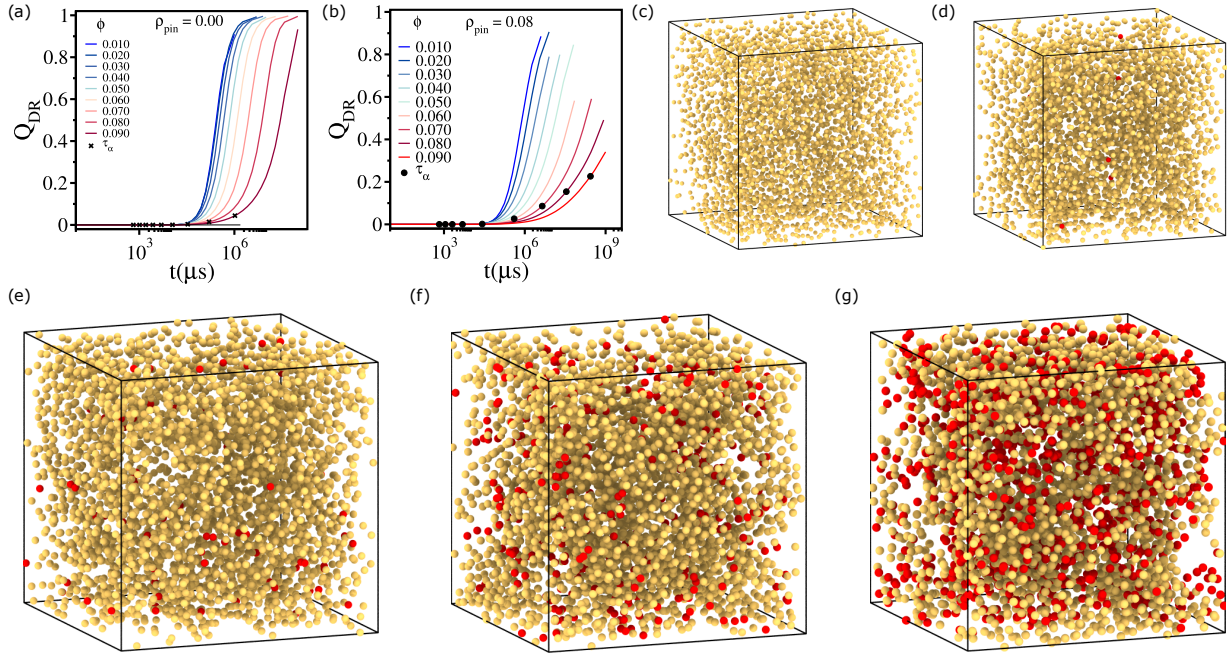


FIG. 7: **Self and distinct correlation:** (a) $Q_{DR} = Q_D/Q_c$ as a function of t for $0.01 \leq \phi \leq 0.09$ with $\rho_{\text{pin}} = 0.0$ for $\rho_r = 0$. The relaxation time at different ϕ is shown as * in the curve. (b) Same as (a) for $\rho_{\text{pin}} = 0.08$. Relaxation time at different ϕ is shown as the black circle in the curves. Simulation snapshots for self-correlated and distinctly correlated particles at $t = \tau_\alpha$ at $\rho_{\text{pin}} = 0.08$ for $\phi = 0.03$ (c), $\phi = 0.05$ (d), $\phi = 0.06$ (e), $\phi = 0.07$ (f) and $\phi = 0.09$ (g). Yellow particles are self-correlated, and red particles are distinctly correlated.

$\tau_\alpha \sim \exp[k\xi_d^c]$. In contrast, in the compressed RFOT-dominated regime, the data is better fit by $\tau_\alpha \sim \exp[k(\xi_d^c)^{3/2}]$. We surmise that the apparent non-monotonic behavior in the dynamic length scale is a consequence of a dynamic crossover, where the collective motion of particles starts to dominate, and activated processes control transport [11]. In unpinned systems, there is no discernible crossover in the dynamics in the studied range of ϕ (Fig. 8 (a)). This is because for an unpinned system, the range of values of ϕ 's that we can reliably simulate is not sufficient enough to explore RFOT behavior. We expect that for the systems in the absence of pinned particles, one might also see such dynamic crossover if the packing fraction is increased, as illustrated in Fig. 7 (a). The biggest and the most significant advantage of the pinning protocol, preferably by self-pinning, is that the crossover to the RFOT-dominated regime may be simulated.

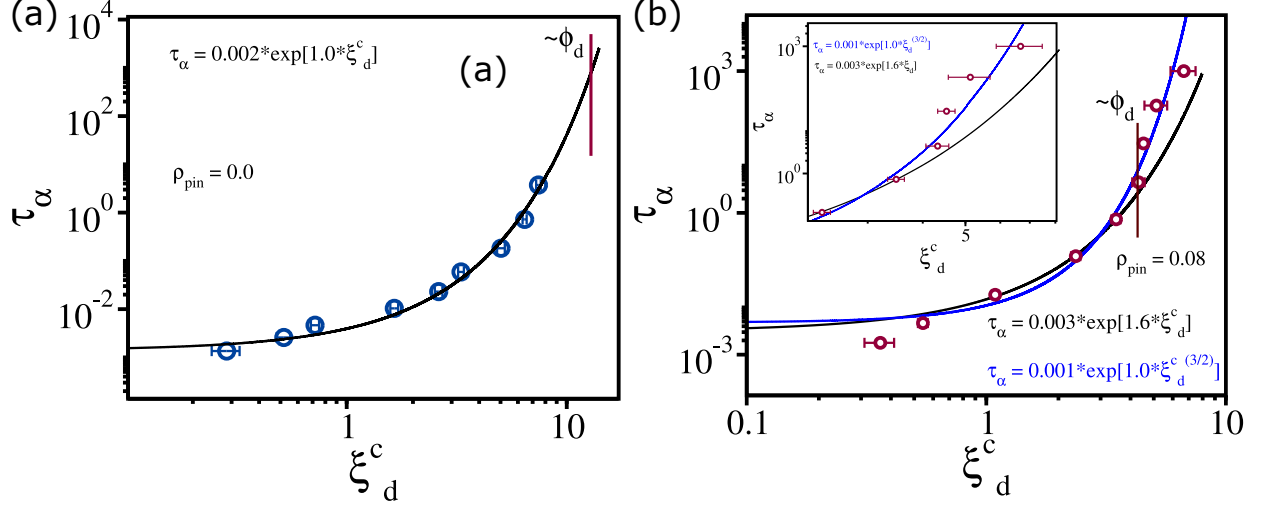


FIG. 8: **Dynamical crossover:** (a) Relaxation time τ_α as a function of dynamic length scales ξ_d^c in a log-log scale for $\rho_r = 0$ with $\rho_{\text{pin}} = 0.0$. The solid black line is fit to $\tau_\alpha \sim \exp(k\xi_d^c)$. The vertical red line indicates the position of ϕ_d [44]. (b) Same as (a), but for $\rho_{\text{pin}} = 0.08$. The blue dashed line is fit to $\tau_\alpha \sim \exp(k(\xi_d^c)^{3/2})$ and the black dashed line is fit to $\tau_\alpha \sim \exp(k\xi_d^c)$. The vertical red line corresponds to the position of ϕ_d . The inset shows the zoomed-in version for better visualization.

Salt effects on the dynamic length: The interaction potential (Eqn. (1)) between charged colloidal particles may be altered by adding monovalent salts. Because salt effects can be probed experimentally, it is of interest to predict the changes in the dynamics at $\rho_r \neq 0$. We performed simulations with $\rho_r = 5$ and 10 (Eqn. (3)) to assess the extent to which ξ_d^c and ξ_d^s change as a function of ϕ . As before, we fit Eqn. (11) and Eqn. (8) to the OZ equation. For $\rho_r = 5$ and $\rho_{\text{pin}} = 0.0$, the ξ_d^s and ξ_d^c grows *monotonically* as a function of ϕ (Fig. 9 (a)). For $\rho_{\text{pin}} = 0.08$, ξ_d^c increases *monotonically* but ξ_d^s grows *non-monotonically* as a function of ϕ (Fig. 9 (b)). It is worth noting that the peak in ξ_d^s is at $\phi \approx 0.35$, which is much higher than the value at $\rho_r = 0$ because ϕ_d depends on the salt concentration (see Table 1 in [44]). It is worth noting that peak in ξ_d^s for $\rho_r = 0$ is much more prominent than for $\rho_r = 5$ (compare Fig. 5 (d) and Fig. 9 (b)). For $\rho_r = 10$, there is a sign of non-monotonicity in ξ_d^s at $\phi \sim 0.44$ (Fig. 9 (c)) although it is not as clear as $\rho_r = 0$ or $\rho_r = 5$. This is because as the salt concentration increases the effective range of interaction potential decreases. Therefore, the effect of pinned particles on the dynamics of unpinned particles will be weaker at high salt concentrations. Thus, one needs to simulate high ρ_{pin} or high packing fractions to see

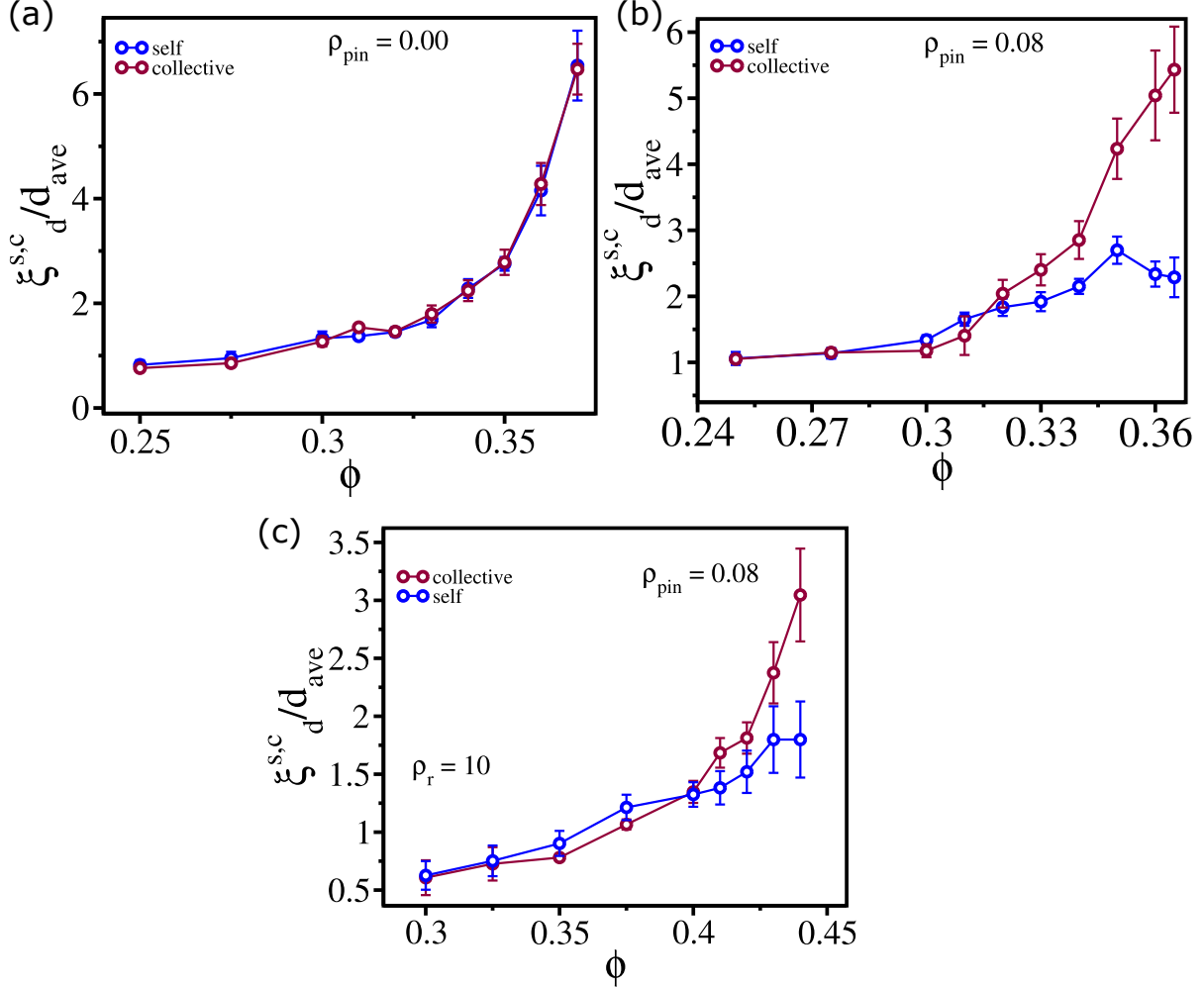


FIG. 9: **Comparison of dynamic length from collective and self-correlation function for $\rho_r = 5$:** Plots of ξ_d^s and ξ_d^c as a function of ϕ for $\rho_r = 5$ using $S_4^s(q, t)$ and $S_{mp}^c(q, t)$ respectively with $\rho_{\text{pin}} = 0.00$ (a) and with $\rho_{\text{pin}} = 0.08$ (b). (c) Same as (b) but for $\rho_r = 10$.

similar prominent peak in ξ_d^s as $\rho_r = 0$.

IV. CONCLUSIONS

We performed Brownian dynamic simulations of a mixture of charged micron-sized colloidal particles to create a consistent method to extract dynamic length in glass forming systems with and without random pinning. Our primary finding is that the collective dynamic length (ξ_d^c), calculated using the small q limit of the multi-point structure factor $S_{mp}^c(q, t)$ (Eqn. (11)), which is well fit to the OZ function at small q , increases monotonically

in both the pinned and unpinned systems. Given this finding, it is worth pondering about the utility of the RP method, especially when a large perturbation like an amorphous wall [31, 37, 38] is used to estimate the dynamic length. Even though the RP method, with different ways of implementing pinning, has provided insights into the nature of the ideal glass transition, the undesired consequences (unknown non-nonlinear response of unpinned particles on the mobile particles and breakage of translational invariance) call into question its ultimate utility. In binary mixture of charged colloidal particles the characteristics of the system change drastically due to the presence of externally imposed disorders. Clearly, the fragility of the system changes by a factor of $\sim 4 - 5$ for 8% pinning (see Fig. 6). Therefore, the length scale obtained by pinning particles is not the length scale associated with the actual liquid under consideration. As shown here and established previously by FS [35], it suffices to extract the dynamic length using Eqn. (11) or Eqn. (10) in the absence of random pinning. We hasten to add that hints in the crossover behavior in the relaxation times to the RFOT-dominated regime can most readily be revealed by probing the dynamics of the constrained liquids by random pinning methods [28].

Because the non-monotonic dependence of ξ_d^s appears when collective dynamics start to become significant, we surmise that the self-four-point dynamic structure factor $S_4^s(q, t)$ underestimates the overall correlation between particles. In contrast, ξ_d^c calculated using multi-particle structure factor $S_{mp}^c(q, t)$ increases *monotonically* as a function of ϕ . It is important to note that, although pinning does decrease the magnitude of ξ_d^s (compare panels (b) and (f) in Fig. 3), the qualitative behavior is unaltered at $\phi < \phi_d$. Collective dynamics, which is accompanied by the change in the shape (fractal to compact) of the cooperative regions [41], is prominent only at volume fraction that exceeds ϕ_d . The crossover in the dynamics, where collective motions of particles become important, is also reflected not only in that shape of the cooperative regions but also in the dependence of the τ_α on the dynamic length. The RFOT-dominated regime ($\tau_\alpha \sim \exp[k(\xi_d^c)^{3/2}]$) appears roughly at the packing fraction where collective dynamics start to emerge.

The prediction that the collective dynamic length may be estimated in the presence or absence of random pinning can be verified in experiments. All it requires is the reanalysis of the video microscopy data reported previously [40] using the method introduced here. Rather than measure single-particle dynamics, it would be necessary to probe correlated dynamics using the order parameter proposed here.

Acknowledgements: DT is grateful to Peter Rossky for discussions on the history of MD simulations of proteins. We are grateful to Hyun W. Cho for help in the early stages of this work. This work was supported by a grant from the National Science Foundation (CHE 2320256) and the Welch Foundation through the Collie-Welch chair (F0019).

Appendix

Calculation of a growing length using $S_{mp}^c(q, t)$

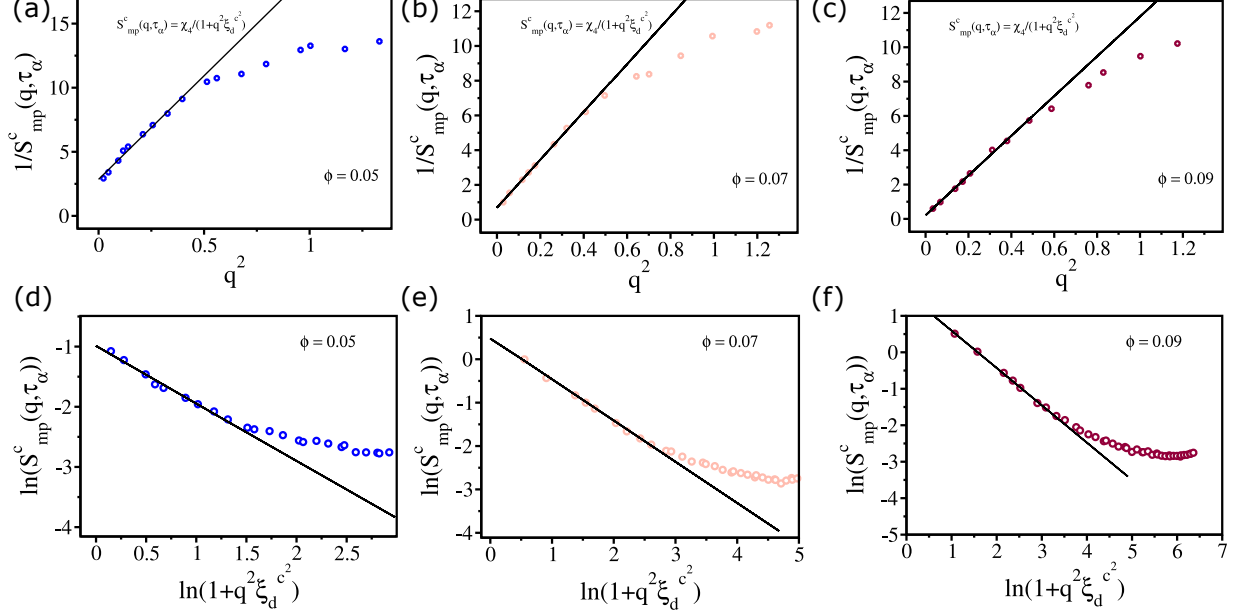


FIG. 10: **Estimation of length scale from $S_4(q, t)$:** (a)-(c) $1/S_{mp}^c(q, \tau_\alpha)$ as a function of q^2 for $\phi = 0.05, 0.07$ and 0.09 respectively. The solid lines are linear fit to the function $1/S_{mp}^c(q, \tau_\alpha) = 1/\chi_4 + q^2 \xi_d^{c2}/\chi_4$. (d)-(e) $\ln(S_{mp}^c(q, \tau_\alpha))$ as a function of $\ln(1 + q^2 \xi_d^{c2})$ for $\phi = 0.05, 0.07$ and 0.09 respectively. The solid lines are linear fit. The results are for $\rho_r = 0$ with $\rho_{pin} = 0.00$.

To demonstrate that ξ_d^c can be reliably calculated from the low- q values of $S_{mp}^c(q, \tau_\alpha)$, we employed two methods. As illustrated in Fig. 10 (a)-(c) (for $\rho_{pin} = 0.0$) and Fig. 11 (a)-(c) (for $\rho_{pin} = 0.08$), the inverse function $1/S_{mp}^c(q, \tau_\alpha)$ plotted as a function of q^2 is linear at low q values, which shows that extrapolating $S_{mp}^c(q, \tau_\alpha)$ to the $q \rightarrow 0$ limit is robust. Specifically, at low q values, at least 6–7 data points were well-fit to a linear function, allowing for accurate calculation of the length scale.

To further validate this approach, we plotted $\ln(S_{mp}^c(q, \tau_\alpha))$ as a function of $\ln(1 + q^2 \xi_d^{c2})$ using the estimated values of ξ_d^c . The low- q data points also showed a strong linear fit to this function, confirming the reliability of the estimation (Fig. 10 (d)-(f) and Fig. 11 (d)-(f)).

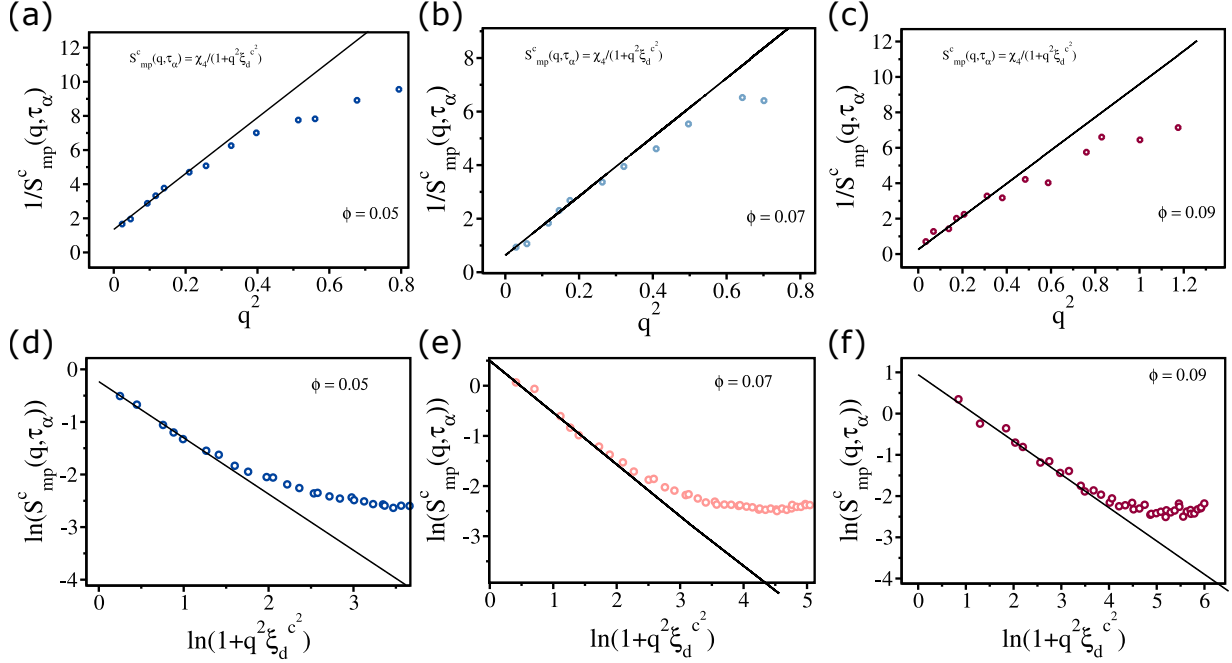


FIG. 11: **Estimation of length scale from $S_4(q, t)$:** (a)-(c) $1/S_{mp}^c(q, \tau_\alpha)$ as a function of q^2 for $\phi = 0.05, 0.07$ and 0.09 respectively. The solid lines are linear fit to the function $1/S_{mp}^c(q, \tau_\alpha) = 1/\chi_4 + q^2 \xi_d^{c^2}/\chi_4$. (d)-(e) $\ln(S_{mp}^c(q, \tau_\alpha))$ as a function of $\ln(1 + q^2 \xi_d^{c^2})$ for $\phi = 0.05, 0.07$ and 0.09 respectively. The solid lines are linear fit. (a)-(f) are for $\rho_r = 0$ with $\rho_{pin} = 0.08$.

The results shown in Fig. 11 are for $\rho_{pin} = 0.0$ and Fig. 11 are for $\rho_{pin} = 0.08$.

-
- [1] Aneesur Rahman. Correlations in the motion of atoms in liquid argon. *Physical review*, 136(2A):A405, 1964.
 - [2] M. Parrinello and A. Rahman. Polymorphic transitions in single crystals: A new molecular dynamics method. *Journal of Applied Physics*, 52(12):7182–7190, 1981.
 - [3] John R. Ray and Aneesur Rahman. Statistical ensembles and molecular dynamics studies of anisotropic solids. II. *The Journal of Chemical Physics*, 82(9):4243–4247, 1985.
 - [4] David JE Callaway and Aneesur Rahman. Microcanonical ensemble formulation of lattice gauge theory. *Physical review letters*, 49(9):613, 1982.
 - [5] Aneesur Rahman and Frank H Stillinger. Molecular dynamics study of liquid water. *The Journal of Chemical Physics*, 55(7):3336–3359, 1971.

- [6] Frank H Stillinger and Aneesur Rahman. Improved simulation of liquid water by molecular dynamics. *The Journal of Chemical Physics*, 60(4):1545–1557, 1974.
- [7] Aneesur Rahman, M. J. Mandell, and J. P. McTague. Molecular dynamics study of an amorphous lennard-jones system at low temperature. *The Journal of Chemical Physics*, 64(4):1564–1568, 1976.
- [8] Sidney R Nagel, A Rahman, and Gary S Grest. Normal-mode analysis by quench-echo techniques: Localization in an amorphous solid. *Physical Review Letters*, 47(23):1665, 1981.
- [9] Peter J Rossky, Martin Karplus, and Aneesur Rahman. A model for the simulation of an aqueous dipeptide solution. *Biopolymers: Original Research on Biomolecules*, 18(4):825–854, 1979.
- [10] Gerold Adam and Julian H. Gibbs. On the temperature dependence of cooperative relaxation properties in glass-forming liquids. *The Journal of Chemical Physics*, 43(1):139–146, 1965.
- [11] T. R. Kirkpatrick, D. Thirumalai, and P. G. Wolynes. Scaling concepts for the dynamics of viscous liquids near an ideal glassy state. *Phys. Rev. A*, 40:1045–1054, 1989.
- [12] T. R. Kirkpatrick and D. Thirumalai. Colloquium: Random First Order Transition theory concepts in biology and physics. *Rev. Mod. Phys.*, 87:183–209, 2015.
- [13] G Tarjus, S A Kivelson, Z Nussinov, and P Viot. The frustration-based approach of supercooled liquids and the glass transition: a review and critical assessment. *Journal of Physics: Condensed Matter*, 17(50):R1143, 2005.
- [14] Chiara Cammarota and Giulio Biroli. Random pinning glass transition: Hallmarks, mean-field theory and renormalization group analysis. *The Journal of Chemical Physics*, 138(12):12A547, 2013.
- [15] Vassiliy Lubchenko and Peter G. Wolynes. Theory of structural glasses and supercooled liquids. *Annual Review of Physical Chemistry*, 58:235–266, 2007.
- [16] B. Bernu, J. P. Hansen, Y. Hiwatari, and G. Pastore. Soft-sphere model for the glass transition in binary alloys: Pair structure and self-diffusion. *Physical Review A*, 36(10):4891, 1987.
- [17] Raymond D. Mountain and D. Thirumalai. Molecular-dynamics study of glassy and supercooled states of a binary mixture of soft spheres. *Physical Review A*, 36(7):3300, 1987.
- [18] J.-L Barrat and Ludovic Bethier. Molecular dynamics simulations of supercooled liquids near the glass transition. *Annu. Rev. Phys. Chem.*, 42:23–53, 1991.
- [19] Walter Kob and Hans C Andersen. Testing mode-coupling theory for a supercooled binary

- lennard-jones mixture I: The van hove correlation function. *Physical Review E*, 51(5):4626, 1995.
- [20] Camille Scalliet, Benjamin Guiselin, and Ludovic Berthier. Thirty milliseconds in the life of a supercooled liquid. *Physical Review X*, 12(4):041028, 2022.
 - [21] J-L Barrat and Ludovic Berthier. Computer simulations of the glass transition and glassy materials. *Comptes Rendus. Physique*, 24(S1):57–73, 2023.
 - [22] T. R. Kirkpatrick and D. Thirumalai. *Universal Aspects of the Structural Glass Transition from Density Functional Theory*, pages 115–133. Spin Glass Theory and Far Beyond. WORLD SCIENTIFIC, 2023.
 - [23] Giulio Biroli and Jean-Philippe Bouchaud. *The Random First-Order Transition Theory of Glasses: A Critical Assessment*, pages 31–113. Structural Glasses and Supercooled Liquids. 2012. Wiley Online Books.
 - [24] Ludovic Berthier and Walter Kob. Static point-to-set correlations in glass-forming liquids. *Phys. Rev. E*, 85:011102, 2012.
 - [25] Smarajit Karmakar and Giorgio Parisi. Random pinning glass model. *Proceedings of the National Academy of Sciences*, 110(8):2752–2757, 2013.
 - [26] Walter Kob and Ludovic Berthier. Probing a liquid to glass transition in equilibrium. *Phys. Rev. Lett.*, 110:245702, 2013.
 - [27] Saurish Chakrabarty, Smarajit Karmakar, and Chandan Dasgupta. Dynamics of glass forming liquids with randomly pinned particles. *Scientific Reports*, 5(1):12577, 2015.
 - [28] Chiara Cammarota and Giulio Biroli. Ideal glass transitions by random pinning. *Proceedings of the National Academy of Sciences*, 109(23):8850–8855, 2012.
 - [29] Saurish Chakrabarty, Rajsekhar Das, Smarajit Karmakar, and Chandan Dasgupta. Understanding the dynamics of glass-forming liquids with random pinning within the Random First Order Transition theory. *The Journal of Chemical Physics*, 145(3):034507, 2016.
 - [30] Misaki Ozawa, Walter Kob, Atsushi Ikeda, and Kunimasa Miyazaki. Equilibrium phase diagram of a randomly pinned glass-former. *Proceedings of the National Academy of Sciences*, 112(22):6914–6919, 2015.
 - [31] Walter Kob, Sándalo Roldán-Vargas, and Ludovic Berthier. Non-monotonic temperature evolution of dynamic correlations in glass-forming liquids. *Nature Physics*, 8(2):164–167, 2012.
 - [32] Jean-Philippe Bouchaud and Giulio Biroli. On the Adam-Gibbs-Kirkpatrick-Thirumalai-

- Wolynes scenario for the viscosity increase in glasses. *The Journal of Chemical Physics*, 121(15):7347–7354, 2004.
- [33] G. Biroli, J.-P. Bouchaud, A. Cavagna, T. S. Grigera, and P. Verrocchio. Thermodynamic signature of growing amorphous order in glass-forming liquids. *Nature Physics*, 4(10):771–775, 2008.
- [34] Glen M. Hocky, Thomas E. Markland, and David R. Reichman. Growing point-to-set length scale correlates with growing relaxation times in model supercooled liquids. *Phys. Rev. Lett.*, 108:225506, 2012.
- [35] Elijah Flenner and Grzegorz Szamel. Characterizing dynamic length scales in glass-forming liquids. *Nature Physics*, 8(10):696–697, 2012.
- [36] Baicheng Mei, Yuyuan Lu, Lijia An, Hongfei Li, and Liang Wang. Nonmonotonic dynamic correlations in quasi-two-dimensional confined glass-forming liquids. *Phys. Rev. E*, 95:050601, 2017.
- [37] Glen M. Hocky, Ludovic Berthier, Walter Kob, and David R. Reichman. Crossovers in the dynamics of supercooled liquids probed by an amorphous wall. *Phys. Rev. E*, 89:052311, 2014.
- [38] K. Hima Nagamanasa, Shreyas Gokhale, A. K. Sood, and Rajesh Ganapathy. Direct measurements of growing amorphous order and non-monotonic dynamic correlations in a colloidal glass-former. *Nature Physics*, 11(5):403–408, 2015.
- [39] T. R. Kirkpatrick and D. Thirumalai. Random solutions from a regular density functional hamiltonian: a static and dynamical theory for the structural glass transition. *Journal of Physics A: Mathematical and General*, 22(5):L149, 1989.
- [40] Divya Ganapathi, K. Hima Nagamanasa, A. K. Sood, and Rajesh Ganapathy. Measurements of growing surface tension of amorphous–amorphous interfaces on approaching the colloidal glass transition. *Nature Communications*, 9(1):397, 2018.
- [41] Jacob D. Stevenson, Jörg Schmalian, and Peter G. Wolynes. The shapes of cooperatively rearranging regions in glass-forming liquids. *Nature Physics*, 2(4):268–274, 2006.
- [42] C. J. Camacho and D. Thirumalai. Kinetics and thermodynamics of folding in model proteins. *Proceedings of the National Academy of Sciences*, 90(13):6369–6372, 1993.
- [43] Zhuyan Guo and D Thirumalai. Kinetics of protein folding: nucleation mechanism, time scales, and pathways. *Biopolymers: Original Research on Biomolecules*, 36(1):83–102, 1995.
- [44] Hyun Woo Cho, Mauro L. Mugnai, T. R. Kirkpatrick, and D. Thirumalai. Fragile-to-strong

- crossover, growing length scales, and dynamic heterogeneity in wigner glasses. *Phys. Rev. E*, 101:032605, 2020.
- [45] H. M. Lindsay and P. M. Chaikin. Elastic properties of colloidal crystals and glasses. *The Journal of Chemical Physics*, 76(7):3774–3781, 04 1982.
 - [46] Hongsuk Kang, T. R. Kirkpatrick, and D. Thirumalai. Manifestation of Random First-Order Transition theory in wigner glasses. *Phys. Rev. E*, 88:042308, 2013.
 - [47] R O Rosenberg, D Thirumalai, and R D Mountain. Liquid, crystalline and glassy states of binary charged colloidal suspensions. *Journal of Physics: Condensed Matter*, 1(11):2109–2114, 1989.
 - [48] S. Alexander, P. M. Chaikin, P. Grant, G. J. Morales, P. Pincus, and D. Hone. Charge renormalization, osmotic pressure, and bulk modulus of colloidal crystals: Theory. *The Journal of Chemical Physics*, 80(11):5776–5781, 1984.
 - [49] R. O. Rosenberg and D. Thirumalai. Order-disorder transition in colloidal suspensions. *Phys. Rev. A*, 36:5690–5700, 1987.
 - [50] Subrata Sanyal and Ajay K. Sood. Brownian dynamics simulation of dense binary colloidal mixtures. I. Structural evolution and dynamics. *Phys. Rev. E*, 52:4154–4167, 1995.
 - [51] D. Thirumalai. Liquid and crystalline states of monodisperse charged colloidal particles. *The Journal of Physical Chemistry*, 93(15):5637–5644, 1989.
 - [52] Michael E. Fisher, Yan Levin, and Xiaojun Li. The interaction of ions in an ionic medium. *The Journal of Chemical Physics*, 101(3):2273–2282, 1994.
 - [53] Elijah Flenner, Min Zhang, and Grzegorz Szamel. Analysis of a growing dynamic length scale in a glass-forming binary hard-sphere mixture. *Phys. Rev. E*, 83:051501, 2011.
 - [54] Bhanu Prasad Bhowmik, Rajsekhar Das, and Smarajit Karmakar. Understanding the stokes–einstein relation in supercooled liquids using random pinning. *Journal of Statistical Mechanics: Theory and Experiment*, 2016(7):074003, 2016.
 - [55] Rajsekhar Das, Saurish Chakrabarty, and Smarajit Karmakar. Pinning susceptibility: a novel method to study growth of amorphous order in glass-forming liquids. *Soft Matter*, 13:6929–6937, 2017.
 - [56] M. D. Ediger. Spatially heterogeneous dynamics in supercooled liquids. *Annual Review of Physical Chemistry*, 51(1):99–128, 2000. PMID: 11031277.
 - [57] Ranko Richert. Heterogeneous dynamics in liquids: fluctuations in space and time. *Journal*

- of Physics: Condensed Matter*, 14(23):R703–R738, 2002.
- [58] T. R. Kirkpatrick and D. Thirumalai. Comparison between dynamical theories and metastable states in regular and glassy mean-field spin models with underlying first-order-like phase transitions. *Phys. Rev. A*, 37:4439–4448, 1988.
 - [59] Cristina Toninelli, Matthieu Wyart, Ludovic Berthier, Giulio Biroli, and Jean-Philippe Bouchaud. Dynamical susceptibility of glass formers: Contrasting the predictions of theoretical scenarios. *Phys. Rev. E*, 71:041505, 2005.
 - [60] Jean-Philippe Bouchaud and Giulio Biroli. Nonlinear susceptibility in glassy systems: A probe for cooperative dynamical length scales. *Phys. Rev. B*, 72:064204, 2005.
 - [61] Ludovic Berthier and Giulio Biroli. Theoretical perspective on the glass transition and amorphous materials. *Rev. Mod. Phys.*, 83:587–645, 2011.
 - [62] Ludovic Berthier, Giulio Biroli, Jean-Philippe Bouchaud, Luca Cipelletti, and Wim van Saarloos. *Dynamical heterogeneities in glasses, colloids, and granular media*, volume 150. OUP Oxford, 2011.
 - [63] Walter Kob and Daniele Coslovich. Nonlinear dynamic response of glass-forming liquids to random pinning. *Phys. Rev. E*, 90:052305, 2014.
 - [64] Yan-Wei Li, You-Liang Zhu, and Zhao-Yan Sun. Decoupling of relaxation and diffusion in random pinning glass-forming liquids. *The Journal of Chemical Physics*, 142(12):124507, 2015.
 - [65] Elijah Flenner and Grzegorz Szamel. Dynamic heterogeneity in a glass forming fluid: Susceptibility, structure factor, and correlation length. *Phys. Rev. Lett.*, 105:217801, 2010.
 - [66] N. Lačević, F. W. Starr, T. B. Schröder, and S. C. Glotzer. Spatially heterogeneous dynamics investigated via a time-dependent four-point density correlation function. *The Journal of Chemical Physics*, 119(14):7372–7387, 2003.
 - [67] Smarajit Karmakar, Chandan Dasgupta, and Srikanth Sastry. Analysis of dynamic heterogeneity in a glass former from the spatial correlations of mobility. *Phys. Rev. Lett.*, 105:015701, 2010.
 - [68] Hailong Peng, Huashan Liu, and Thomas Voigtmann. Nonmonotonic dynamical correlations beneath the surface of glass-forming liquids. *Phys. Rev. Lett.*, 129:215501, 2022.
 - [69] Robert L Jack and Christopher J Fullerton. Dynamical correlations in a glass former with randomly pinned particles. *Physical Review E*, 88(4):042304, 2013.
 - [70] Misaki Ozawa, Walter Kob, Atsushi Ikeda, and Kunimasa Miyazaki. Reply to chakrabarty

- et al.: Particles move even in ideal glasses. *Proceedings of the National Academy of Sciences*, 112(35):E4821–E4822, 2015.
- [71] Raymond D. Mountain and D. Thirumalai. Quantitative measure of efficiency of monte carlo simulations. *Physica A: Statistical Mechanics and its Applications*, 210(3):453–460, 1994.